Title

Influence of landscape heterogeneity on water available to tropical forests in an Amazonian catchment and implications for modeling drought response

Journal

Journal of Geophysical Research: Atmospheres, 122(16)

ISSN

2169-897X

Authors

Fang, Yilin
Leung, L Ruby
Duan, Zhuoran
et al.

Publication Date

2017-08-27

DOI

10.1002/2017jd027066

Peer reviewed

Influence of landscape heterogeneity on water available to tropical forests in an Amazonian catchment and implications for modeling drought response

Yilin Fang

L. Ruby Leung

Zhuoran Duan

Mark S. Wigmosta

Reed M. Maxwell

Jeffrey Q. Chambers
Javier Tomasella
First published: 07 August 2017

https://doi.org/10.1002/2017JD027066

Abstract

The Amazon basin has experienced periodic droughts in the past, and intense and frequent droughts are predicted in the future. Landscape heterogeneity could play an important role in how tropical forests respond to drought by influencing water available to plants. Using the one-dimensional ACME Land Model and the three-dimensional ParFlow variably saturated flow model, numerical experiments were performed for a catchment in central Amazon to elucidate processes that influence water available for plant use and provide insights for improving Earth system models. Results from ParFlow show that topography has a dominant influence on groundwater table and runoff through lateral flow. Without any representations of lateral processes, ALM simulates very different seasonal variations in groundwater table and runoff compared to ParFlow even if it is able to reproduce the long-term spatial average groundwater table of ParFlow through simple parameter calibration. In the ParFlow simulations, even in the

plateau with much deeper water table depth during the dry season in the drought year of 2005, plant transpiration is not water stressed as the soil saturation is still sufficient for the stomata to be fully open based on the empirical wilting formulation in the models. This finding is insensitive to uncertainty in atmospheric forcing and soil parameters, but the empirical wilting formulation is an important factor that should be addressed using observations and modeling of coupled plant hydraulics-soil hydrology processes in future studies. The results could be applicable to other catchments in the Amazon basin with similar seasonal variability and hydrologic regimes.

1 Introduction

As the largest tropical rainforest in the world, Amazonia in South America plays a crucial role in the global energy, water, and carbon cycles [*Cox et al.*, 2004; *Baker et al.*, 2008]. The diabatic heating associated with the clouds and precipitation in the Amazon is a significant forcing for the large-scale atmospheric circulation that influences global climate through teleconnection worldwide [*Medvigy et al.*, 2013]. Rainfall in the Amazon has a notable seasonality associated with the seasonal migration of the tropical rain belt. The Amazonia rainfall also exhibits large interannual variability driven by atmospheric circulation anomalies associated with the El Niño [*Marengo*, 1992; *Rao et al.*, 1996], warm waters in the tropical North Atlantic [*Marengo et al.*, 2011], and other climate modes of variability that resulted in several extreme droughts over the past decades [*Bonal et al.*, 2016]. In response to perturbations by greenhouse gases, aerosols, and land use and land cover change, some climate models projected an increase in the length of the dry season and the area in Amazonia affected by mild and severe meteorological drought in the 21st century [*Boisier et al.*, 2015; *Duffy et al.*, 2015].

The forest vegetation depends on precipitation and soil moisture storage to sustain sufficient transpiration for the plants to remain functional during the dry season or droughts. Runoff, groundwater storage, and surface water-groundwater interactions that influence soil moisture are also likely to influence evapotranspiration in the tropical forest during the dry season [*Miguez-Macho and Fan*, 2012] and in a warmer and drier future climate [*Pokhrel et al.*, 2014]. However, due to the lack of observations and the challenges in modeling hydrological processes, there is a need to improve understanding and characterization of the spatial and temporal patterns of surface and subsurface water available to plants in tropical forests [*Fan et al.*, 2013]. Water available to plants might mitigate or intensify drought effects on plants, but it could vary spatially with landscape heterogeneity. For example, *Daws et al.* [2002] studied the effects of topographic position on water regime in a tropical forest on Barro Colorado Island (BCI) in Panamá using measured soil matric potential and a simple water balance model. They found large variations in water regime over small spatial scales. They suggested that the slope sites on

BCI, buffered against drought by available water, might continue to provide a suitable habitat for moisture demanding species.

A few studies highlighted the importance of both lateral surface and subsurface flow in accurate prediction of the water cycle. Using model results and observations, *Maxwell and Condon* [2016] showed that water table depth and lateral flow strongly affect the partitioning of evapotranspiration into bare soil evaporation and plant transpiration. *Kim and Mohanty*[2016] found surface topography to be a crucial control in representing the variation of near-surface soil moisture, and including lateral subsurface flow can better characterize the spatially distributed patterns of soil moisture in models. *Choi et al*. [2013] significantly improved stream discharge prediction by substituting the one-dimensional (1-D) scheme in the Common Land Model with a conjunctive surface-subsurface flow parameterization. A recent literature review by *Fatichi et al*. [2016] showed the necessity for process-based models for improved understanding of land-atmosphere coupling hotspot regions that are sensitive to land surface heterogeneity and dynamics of atmospheric conditions. However, current land surface models (LSMs) in Earth system models (ESMs) represent moisture transport in a 1-D vertical soil column on computational grids that typically vary between 1/8° to 1° resolution and neglect lateral exchanges of water at the grid or subgrid scales. Although different approaches have been used to represent subgrid heterogeneity, most land models have a simplistic representation of the topographic controls on fine-scale soil moisture heterogeneity so the topographic influence on water available to plants is not adequately captured to simulate the spatial and temporal variation in evapotranspiration (ET).

In central Amazonia, topography is a key driver of groundwater table depth [*Fan et al.*, 2013]. Groundwater table plays a key role in sustaining streamflow and evaporation to buffer intraseasonal-to-interannual rainfall variability [*Tomasella et al.*, 2008]. Observations [see *Fan and Miguez-Macho*, 2010, and references therein] suggested that the Amazon forest as a whole is not water stressed in the dry season. Ensemble LSM simulations performed by *Getirana et al*. [2014] also indicated that ET over most of the Amazon basin does not depend on water availability. Compared to normal climatological years, a recent field study of deep soil water dynamics at a plateau area 30 m from the flux tower K34 showed that roots of the forests at that location could tap into soil water deeper than 4.8 m during the drought year 2005 to satisfy transpiration demand [*Broedel et al.*, 2017], consistent with previous findings of the important role of deep roots in the hydrological cycle of Amazonian forests [*Nepstad et al.*, 1994]. However, systematic investigations on the processes that control water available to plants using process-based models that more realistically simulate surface and subsurface processes are

limited. While overall the Amazon forest is not water stressed in the dry season, it is not clear how landscape heterogeneity modulates surface and subsurface hydrology and water available to plants, leading to different drought responses at the landscape scale.

In this paper, we present results from a set of hydrological modeling experiments in a small central Amazonian catchment, focusing on model structures and processes that are important for water available for plant use in tropical systems. These experiments were designed by using a 1-D land model and a three-dimensional (3-D) variably saturated flow model, varying options of the hydrologic schemes and varying model parameters related to soil and the meteorological forcing. The goals of the study are to (1) elucidate the role of landscape heterogeneity and lateral flow and understand how different hydrological modeling approaches on groundwater storage and evapotranspiration may lead to different plant responses to drought in tropical forest, and (2) provide insights for improving hydrologic modeling in ESMs for projecting tropical forest response to future warming and the implications to the carbon cycle. With the focus on improving understanding of processes and modeling, none of the simulations in this study are formally calibrated to best reproduce the observations, but comparison with limited observation data shows that the hydrologic simulations capture reasonable hydrologic behaviors in the study catchment.

2 Methodology

2.1 Study Site

The study site is the Asu catchment, a small central Amazonian watershed that is located 80 km to the northwest of Manaus (3°08′S, 60°07′W). The wet season in Central Amazonia is from November to May, and the dry season is from June to October. This site contains pristine tropical rainforest, dominated by broadleaf evergreen trees. A more detailed description and characterization of the site can be found in *Cuartas et al*. [2012]. Figure 1a shows the topography of the Asu catchment as determined using data from the 90 m Digital Elevation Model (DEM) derived from the Shuttle Radar Topography Mission. Figure 1b shows the distribution of four soil classes in the catchment at the same 90 m resolution as the topography. The four soil classes, namely, Soil 1, Soil 2, Soil 3, and Soil 4, were derived using a terrain model developed by *Nobre et al*. [2011] for the Asu catchment from four terrain classes: waterlogged, ecotone, slope, and plateau, respectively. The fractions of Soil 1, 2, 3, and 4 are 0.31, 0.18, 0.07, and 0.44, respectively. The plateau soil is composed mostly of clays. A representative set of relevant soil parameters for these four soil classes were calibrated for hydrologic modeling in *Cuartas et al*.

[2012] by minimizing the differences between the observed and simulated soil moisture, water table, and discharge.

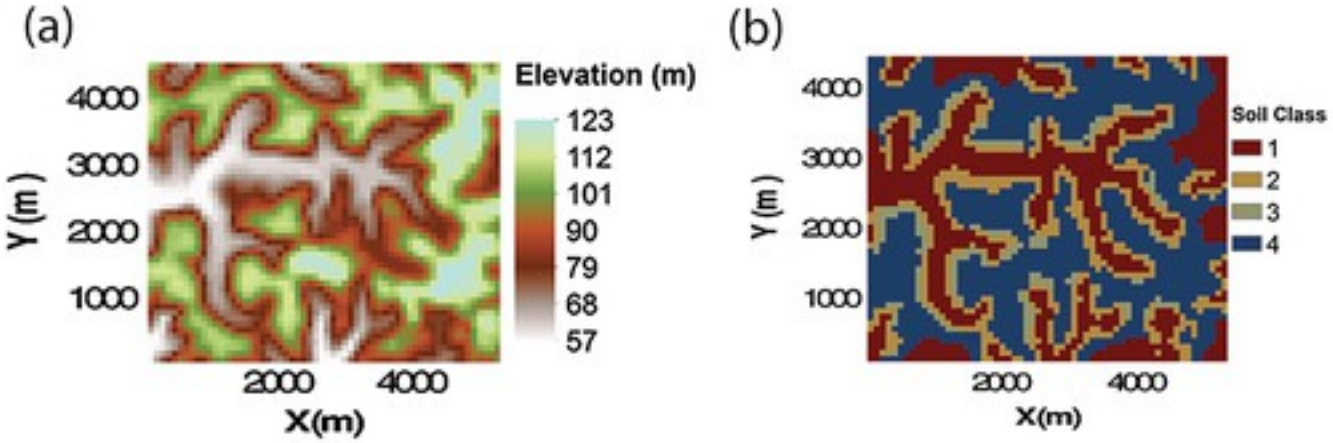

Figure 1
Open in figure viewerPowerPoint
Map of surface elevation and top soil class in the Asu catchment at 90 m resolution. The domain size is 5400 m × 4590 m.

2.2 Numerical Models

Two hydrologic models are compared to provide insights on hydrological processes that affect water available to plants. The first model is the Department of Energy Accelerated Climate Modeling for Energy (ACME) Land Model (ALM). ALM is representative of 1-D models typically used in Earth system models. The second model is ParFlow [*Maxwell et al.*, 2015], which is a 3-D model used to simulate detailed subsurface hydrological processes.

ALM started as a branch of the Community Land Model version 4.5 (CLM4.5) [*Oleson et al.*, 2013]. The default soil hydrology model in ALM is the same as CLM4.5, which solves the 1-D Richards' equation in 10 unevenly spaced vertical soil layers. The layer thicknesses exponentially increase with depth, with the depth of the tenth layer at 3.8 m below the surface. The Richards' equation is expressed as

$$\frac{\partial \theta}{\partial t} = -\frac{\partial q}{\partial z} + Q \quad (1)$$

where θ is the volumetric soil water content, t is time (s), z is elevation in the soil column (m) (positive upward), q is soil water flux (m s^{-1}) (positive upward), and Q is the source/sink term (m m^{-1} s^{-1}). Soil water flux can be solved by Darcy's law expressed as

$$q = -kk_r \frac{\partial(\psi + z)}{\partial z} \quad (2)$$

where k is the saturated hydraulic conductivity, k_r is the relative permeability, and ψ is the soil matric potential (m). Both k_r and ψ vary with volumetric soil water content. In ALM, they are represented by a simplified Brooks and Corey relationship [*Brooks and Corey*, 1966] as follows:

$$\frac{\theta - \theta_r}{\phi - \theta_r} = \left(\frac{\psi_a}{\psi}\right)^{\lambda} \quad (3)$$

$$k_r = \left(\frac{\theta - \theta_r}{\phi - \theta_r}\right)^{n} \quad (4)$$

where θ_r is the residual water content, ϕ is the effective porosity of the media, λ is the pore size distribution index, ψ_a is the bubbling capillary pressure, and n is the pore disconnectedness index. In ALM, $n = 3 + 2/\lambda$.

The θ-based Richards' equation does not account for the variation of pressure head in the saturated zone [*Celia et al.*, 1990]. Therefore, ALM uses a modified Richards' equation derived in *Zeng and Decker* [2009] to maintain the hydrostatic equilibrium soil moisture distribution such that the solution is applicable for variably saturated conditions. The solution, which is the set of soil moisture values for the soil layers, is governed by precipitation, infiltration (i.e., the water that does not run off), subsurface runoff, evaporation, canopy transpiration through root extraction, and interactions with groundwater. In ALM, surface and subsurface runoff or baseflow are parameterized based on the SIMTOP scheme [*Niu et al.*, 2005]. Subsurface runoff follows an exponential decay with respect to water table depth. Treatment of soil column-groundwater interactions is dependent on the water table depth (WTD). When WTD is below the tenth soil layer, an additional layer is added to the bottom layer, with a thickness calculated between the bottom of the tenth layer and the water table. Soil moisture transport is then solved for 11 layers with a zero flux boundary condition applied at the bottom. When WTD is within the 10 soil layers, a zero-flux boundary condition is applied at the bottom of the tenth layer to solve the equations. ALM is available upon request.

ParFlow solves the mixed form of Richards' equation in variably saturated soils in 3-D in the form of equation 5 using a parallel, globalized Newton method and a multigrid preconditioned linear solver [*Ashby and Falgout*, 1996; *Jones and Woodward*, 2001].

$$\frac{\partial \rho s \theta}{\partial t} - \nabla\left[\frac{k k_r \rho}{\mu}, (\nabla p - \rho g \nabla z)\right] = q_s \quad (5)$$

where ρ is the water density (kg m^{-3}), p is the pressure (Pa), s is the water saturation, μ is the viscosity (Pa·s), q_s is the source term (kg m^{-3} s^{-1}), and the rest are the same as in equations 1and 2. The saturation-pressure function and relative permeability-saturation function follow the Brooks and Corey relationships in equations 3 and 4.

Given initial and boundary conditions, ParFlow solves water pressure and the soil water content in the subsurface. The water table depth can be calculated from the pressure of the saturated

region near the ground surface. ParFlow has an integrated surface and subsurface flow simulation capability, where a free-surface overland flow boundary condition is applied at the land surface, and overland flow is solved with the kinematic wave equation [*Kollet and Maxwell*, 2006]. Pressure continuity is assigned at the top boundary between the surface and subsurface systems. The kinetic wave equation is active only when the top cell of the subsurface domain is ponded [*Maxwell et al.*, 2016]. One of the model options is to utilize the terrain following grid (TFG) [*Maxwell*, 2013] capability to define the gridded domain to conform to topography, which is useful for coupled surface-subsurface flow problems. Coupling to an earlier version (version 3.5) of CLM, ParFlow can incorporate physical processes related to the energy and mass balance at the land surface [*Kollet and Maxwell*, 2008]. In the coupled CLM-ParFlow mode, CLM is treated in a distributed manner with a parallel input/output file structure and it is called as a subroutine within ParFlow, with its soil hydrology replaced by the ParFlow 3-D simulation. ParFlow is an open source model, freely available via the GNU LPGL license agreement. Version 3.2 was used in this study and it can be downloaded at https://github.com/parflow/parflow/releases/.

2.3 Forcing and Soil Data

In this study, ALM is run offline with observed atmospheric forcing including surface temperature, pressure, wind velocity, precipitation rate, radiation, and humidity provided as input. The vegetation type is broadleaf evergreen tree. The hourly precipitation rate for 2002–2005 is available from the integrated eddy flux database of Large-scale Biosphere-Atmosphere experiment in Amazonia (LBA) [*Restrepo-Coupe et al.*, 2013]. The average precipitation is 2328 mm per year but 2005 experienced an anomalously dry season with an annual precipitation of 1965 mm under the influence of above normal sea surface temperatures in the tropical North Atlantic [*Marengo et al.*, 2008]. The rest of the meteorological data are from the 0.25°, 3-hourly resolution Princeton's Global Meteorological Forcing Data set, a combination of reanalysis data with observations and disaggregation by statistical downscaling to provide finer resolution in time and space [*Sheffield et al.*, 2006]. In one of the sensitivity test experiments to be described later, all variables of the meteorological forcing are derived from the LBA eddy flux database to determine the sensitivity of our modeling results to uncertainty in meteorological forcing data.

In ALM, soil hydraulic properties (equations 3 and 4) are determined based on percentages of clay, sand, and organic matter content [*Lawrence and Slater*, 2008] that were extracted from the standard CLM surface data set. Soil properties from ALM and *Cuartas et al.* [2012] (referred to as the C12 soils hereafter) for zones between depth 0–0.4 m, 0.4–1.8 m, 1.8–4.8 m, and 4.8–40.0 m are listed in Table 1. The C12 soils have a higher air entry pressure, a narrower range of

pore sizes (indicated by larger λ), and relatively high horizontal saturated conductivity (except for the valley) than the ALM soil. Vertical hydraulic conductivity of the C12 soils gradually decreases with depth. Soil depths for ALM and ParFlow simulations are 48 m and 50 m, respectively. ALM has 15 layers by default, with grid cell depths ranging from 0.017 m at the surface to 13.9 m at the bottom. ParFlow has 27 layers, with grid thickness varying from 0.4 m at the surface to 2 m at the bottom. The watershed is assigned no-flow boundaries on the sides and bottom. The Manning roughness coefficient is 5.52×10^{-5} h $m^{-1/3}$. This coefficient is comparable to values used in other ParFlow applications [e.g., *Maxwell et al.*, 2015] and of the same order as the maximum reported in other studies of the Amazon Basin [see *Luo et al*., 2017, and references therein].

Table 1. Asu Catchment Soil Parameters Based on ALM and C12 for Zones at Different Depth, Surface Zone at the Top for Each Parameter

Parameter	**ALM Soil**	**C12 Soil Class**			
		Waterlogged	**Ecotone**	**Slope**	**Plateau**
Porosity, ϕ (cm^3 cm^{-3})	0.458[a]	0.34	0.32	0.50	0.62
	0.449	0.34	0.36	0.48	0.60
	0.435	0.56	0.43	0.48	0.60
	0.435	0.56	0.43	0.48	0.60
Residual water content, θ_r (cm^3 cm^{-3})	0.0	0.008	0.008	0.12	0.24
	0.0	0.022	0.12	0.16	0.32

Parameter	ALM Soil	C12 Soil Class			
		Waterlogged	Ecotone	Slope	Plateau
	0.0	0.26	0.12	0.18	0.34
	0.0	0.26	0.12	0.18	0.34
Pore size distribution index, λ (-)	0.120	0.78	0.75	0.54	0.35
	0.116	0.85	0.66	0.54	0.29
	0.118	0.28	0.58	0.52	0.28
	0.118	0.28	0.58	0.52	0.28
Bubbling capillary pressure, ψ_a (m)	0.333	0.52	0.56	0.88	0.80
	0.288	0.58	0.72	0.92	0.98
	0.207	1.02	0.74	0.98	1.05
	0.207	1.02	0.74	0.98	1.05
Vetical hydraulic conductivity, K_v ($\times 10^{-4}$ m s^{-1})	0.024	2.488	2.294	0.386	0.598

Parameter	ALM Soil	C12 Soil Class			
		Waterlogged	Ecotone	Slope	Plateau
	0.027	2.364	0.670	0.0054	0.0160
	0.042	0.047	0.210	0.050	0.0018
	0.042	0.047	0.210	0.050	0.0018
Ratio of horizontal to vertical hydraulic conductivity (K_h/K_v)	1.0	0.3329	0.8659	1.594	1.579
	1.0	0.00248	1.551	111.708	58.478
	1.0	6.94×10^{-7}	1.015	11.494	508.495
	1.0	2.73×10^{-14}	0.109	10.737	492.974

- a The four numbers within each parameter category are for depth 0–0.4 m, 0.4–1.8 m, 1.8–4.8 m, and 4.8–40.0 m, respectively.

3 Simulations and Results

3.1 Numerical Experiments Design

Table 2 summarizes six numerical experiments that were conducted to study the hydrological response of the Asu catchment to atmospheric forcing using different models, model structures, and soil properties. Cases 1 and 2 were performed with ALM using the two sets of soil parameters, ALM and the C12 soil at the plateau, respectively. Cases 3 and 4 were performed using ParFlow in the water balance mode driven by the daily net surface water flux (P-ET) simulated by ALM as upper boundary conditions. Case 3 used the ALM soil parameters; Case 4 used the parameters for the C12 soils. Cases 5 and 6 were performed using ParFlow in the energy balance mode when coupled to CLM. Cases 5 and 6 were run using the ALM and C12 soil parameters, respectively. Cases 1–4 will provide insights on the impacts of soil parameters (ALM versus C12) and lateral processes (ALM versus ParFlow driven by the ALM simulated P-ET). Comparisons of Case 5 with Case 3, and Case 6 with Case 4, will elucidate how spatially heterogeneous recharge influence groundwater table and runoff.

Table 2. Numerical Experiments to Evaluate the Impacts of Soil Parameters, Soil Hydrology, and Lateral Processes

Case Number	Model	Driving Force	Soil Parameters
1	ALM, default soil hydrology	Atmospheric forcing[a]	ALM soil
2	ALM, default soil hydrology	Atmospheric forcing	C12 plateau soil
3	ParFlow	P-ET from Case 1[b]	ALM soil
4	ParFlow	P-ET from Case 2	C12 soils
5	CLM-ParFlow	Atmospheric forcing	ALM soil
6	CLM-ParFlow	Atmospheric forcing	C12 soils

- a Atmospheric forcing includes precipitation, temperature, specific humidity, wind speed, surface air pressure, and solar radiation.
- b P-ET is applied at the top boundary of the domain.

All ALM simulations were spun up for 40 years (10 cycles of 2002–2005) and ParFlow simulations were spun up for 4 years using the 2002–2005 forcing to establish the initial conditions. Tests of longer simulation of ALM and ParFlow showed that 4 years of spin-up was enough to reach a dynamic equilibrium. Therefore, another 4 year simulation of 2002–2005 for each case was executed for analysis. Note that ParFlow simulation time is much longer than that of ALM. The ParFlow domain was defined using the terrain following grid method.

A set of sensitivity experiments was performed using ParFlow to evaluate uncertainty of the simulations to several factors that are important for representing water available to plants. These factors include bedrock depth, which affects the total soil water storage, anisotropic ratio of hydraulic conductivity which influences the partitioning of water fluxes between vertical and lateral components and hence, the spatial distribution of groundwater table depth, and lastly atmospheric forcing, which provides constraints on the water and energy input to the system. Although not exhaustive, these sensitivity experiments provide useful insights on the two key questions of the study: (1) what processes influence water available to tropical forest in the Asu catchment, and (2) is the model's ability to answer the first question influenced by uncertainty in hydrologic models? Analyses of the sensitivity experiments will be presented in section 3.5.

3.2 ALM Simulation Results

Figure 2 shows the average time series of observed precipitation and solar radiation and ET simulated by ALM with the default hydrology option (Case 1) and from the CLM-ParFlow simulation (Case 5), both using ALM soil parameters. Figure 3 shows the seasonal variation of the ALM simulated water table depth (WTD) and runoff for Cases 1 and 2. ET exhibits very small seasonal variations. Averaged over the modeling domain, it is slightly higher in the dry season when the net shortwave radiation increases under less cloudy conditions, suggesting that the dry season ET at the Asu catchment as a whole is not controlled by surface water supply, while the wet season ET is limited by radiation. Hence, differences in soil parameters that influence water availability have almost no effect on ET. However, soil parameters have evident effects on WTD (Figure 3a) and runoff (Figure 3b). Case 2 features slightly delayed peak arrival time of WTD and runoff relative to Case 1.

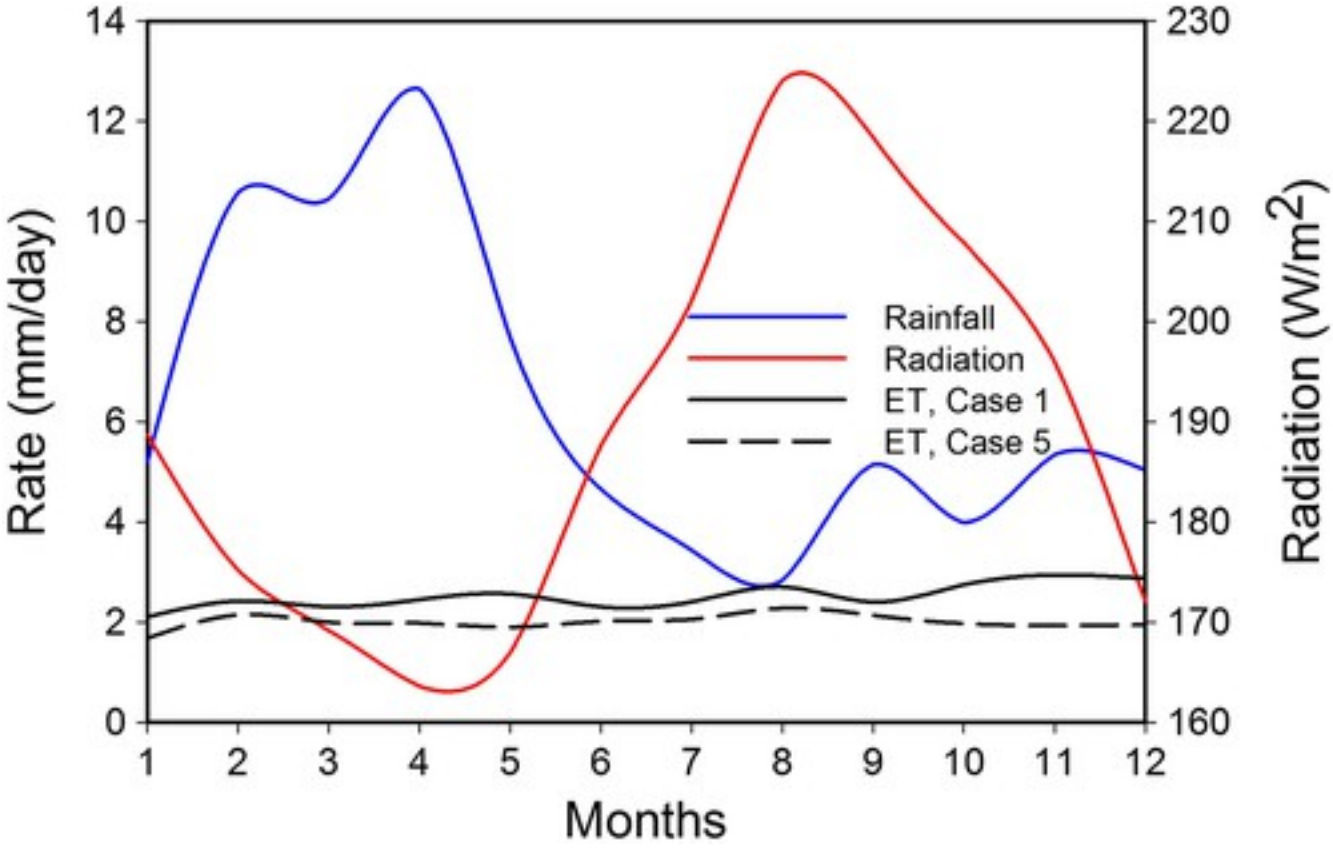

Figure 2

Open in figure viewerPowerPoint

Four year average of rainfall, radiation, and ET simulations from Case 1 and 5.

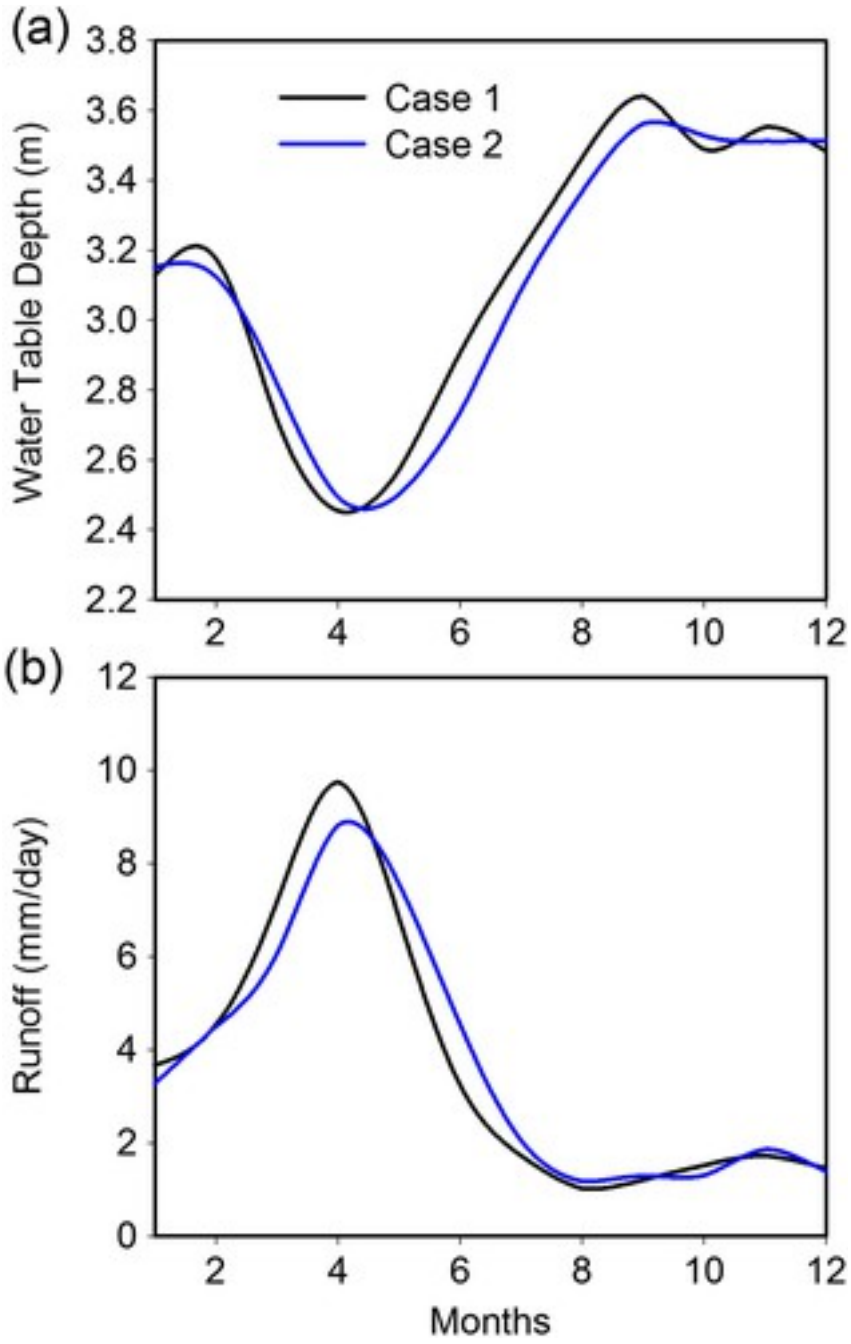

Figure 3

Open in figure viewerPowerPoint

ALM simulations of (a) water table depth and (b) runoff for Cases 1 and 2, averaged over 2002 to 2005.

The simulations show that about 15 to 20% of precipitation contributes to runoff. A significant amount of subsurface flow contributes to runoff during the wet season. In the simulations with the default hydrology option of ALM, the difference between recharge and drainage is scaled by the specific yield of the layer containing the water table to estimate the change in water table.

The specific yield is calculated as equation 6, similar to the expression introduced by *Duke* [1972]:

$$S_y = (\phi - \theta_r)\left(1 - \left(1 + \frac{d}{\psi_a}\right)^{-\lambda}\right) \quad (6)$$

where S_y is the specific yield, θ_r is the residual water content, ϕ is the effective porosity of the media, λ is pore size distribution index, ψ_a is bubbling capillary pressure, and d is water table depth. The specific yield expression in equation 6 has been found to be invalid when the water table fluctuation is large compared to the initial water table depth [*Nachabe*, 2002]. This will affect the parameterization of subsurface runoff as it follows an exponential decay with respect to water table depth. Therefore, a more rigorous approach, such as that solving the variably saturated flow problem, is necessary to estimate the water table depth. The variably saturated flow option is under development in ALM.

3.3 ParFlow Simulation Results

The ParFlow results are spatial averages over the modeling domain shown in Figure 1 unless specified otherwise. Figure 4 shows the various ParFlow simulations of water table depth and runoff compared to the ALM simulation in Case 1. All ParFlow simulations (Cases 3 to 6) predict larger water table depth compared to the ALM simulation. Comparing Cases 1 and 3, the long-term average of WTD from the ALM simulation is 2.5 m shallower than that simulated by ParFlow, and the peak arrival time of groundwater is about 2 months earlier for the ALM simulation. Given the same soil parameters used in the simulations and the surface water infiltration (P-ET) simulated by ALM used as the upper boundary condition for the ParFlow simulations, these results suggest that lateral processes, which are represented in ParFlow but not in ALM could have significant impacts on WTD and its seasonal variability.

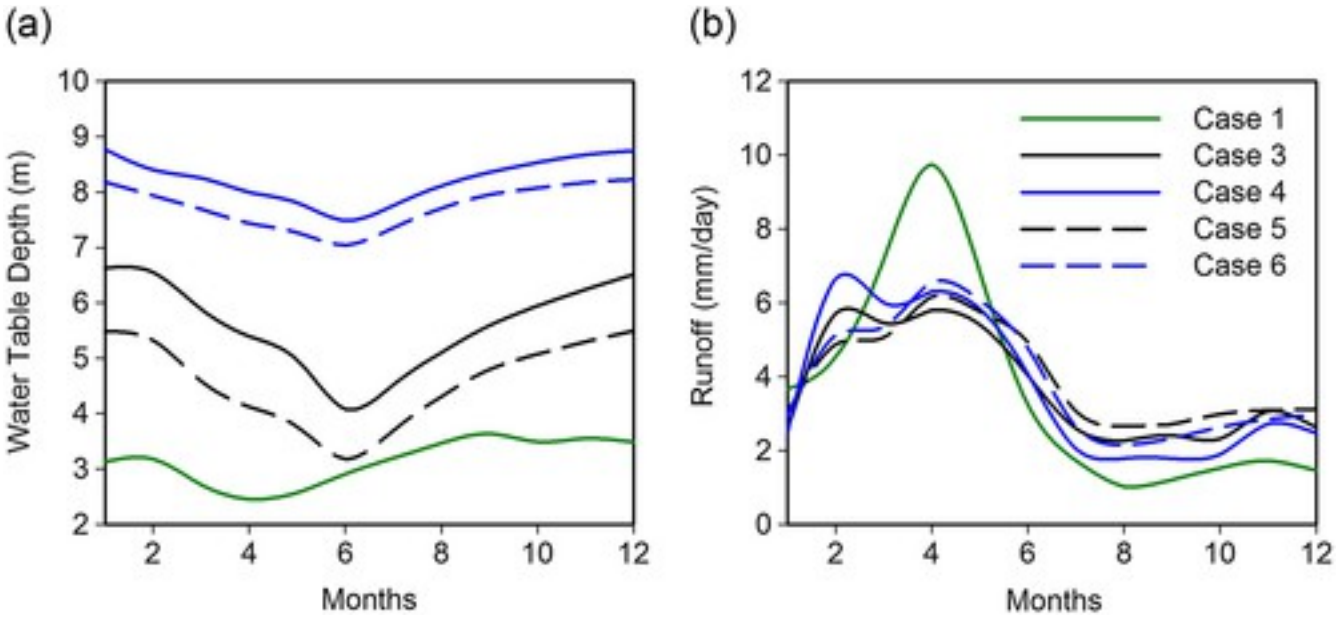

Figure 4

Open in figure viewerPowerPoint

Simulations of (a) water table depth and (b) runoff for Case 1 and Cases 3 to 6, averaged over 2002 to 2005.

Cases 3 and 4 are ParFlow simulations both using P-ET from the ALM simulation, but they differ in the soil parameters used. The long-term average WTD using the ALM soil (Case 3, solid black line in Figure 4a) is 2.6 m shallower than using the C12 soil (Case 4, solid blue line in Figure 4a). Compared to the ALM soil parameters, the horizontal hydraulic conductivity of C12 is greater than the vertical hydraulic conductivity, which enhances the process of subsurface lateral flow. The WTD at the plateau and slope is much lower for Case 4 compared to Case 3 (not shown), which drives the lower average WTD. Case 4 has smaller seasonal variation in WTD compared to Case 3 (Figure 4a). The smaller water table fluctuations of Case 4 are due to the higher lateral conductivity of the C12 soil and the slow vertical drainage at the plateau and slope areas.

Figure 5 shows the spatial distributions of the seasonal variation in WTD (i.e., WTD on 15 April minus WTD on 2 September) in Cases 3 and 4. The plateau areas show larger seasonal variations of WTD than the valley, but plateau and slope regions show smaller WTD during the dry season (September) than the wet season (April). Comparing Cases 3 and 4, the seasonal variations of WTD are again larger in the former, especially at the plateau, which is due to the higher lateral conductivity and the slow vertical drainage of the C12 soil as discussed earlier. In the areas between the plateau and valley, the seasonal variations of WTD can be opposite to that of the plateau. This is also shown in the interannual variability in water table depth at y = 2835 m, 2745 m, 1035 m, and 1485 m, respectively, for the four terrain classes in the cross section

at x = 2295 m for Case 3 (Figure 6). Clear delay of groundwater peak arrival time can be seen in the plateau and slope area due to the differences in the recharge dynamics between the plateau and valley. Because of the deeper water table depth at those areas, it takes longer for the vertical drainage to reach the water table.

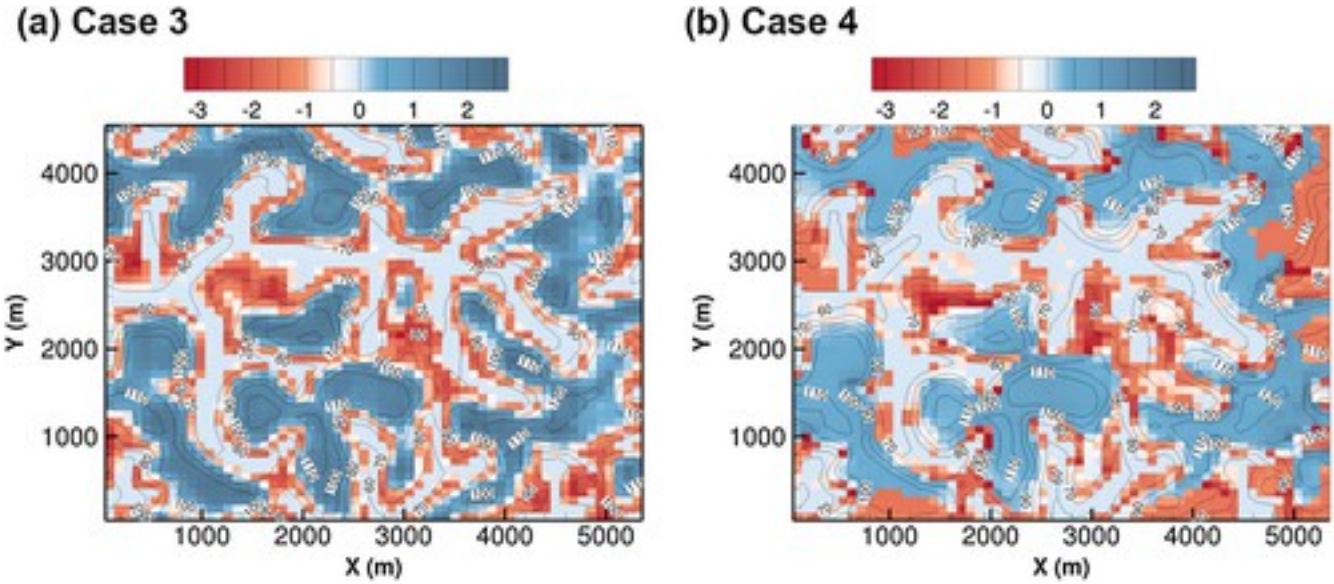

Figure 5
Open in figure viewerPowerPoint
Spatial plot of water table difference (m) between 15 April and 2 September in 2005 for (a) Case 3 and (b) Case 4.

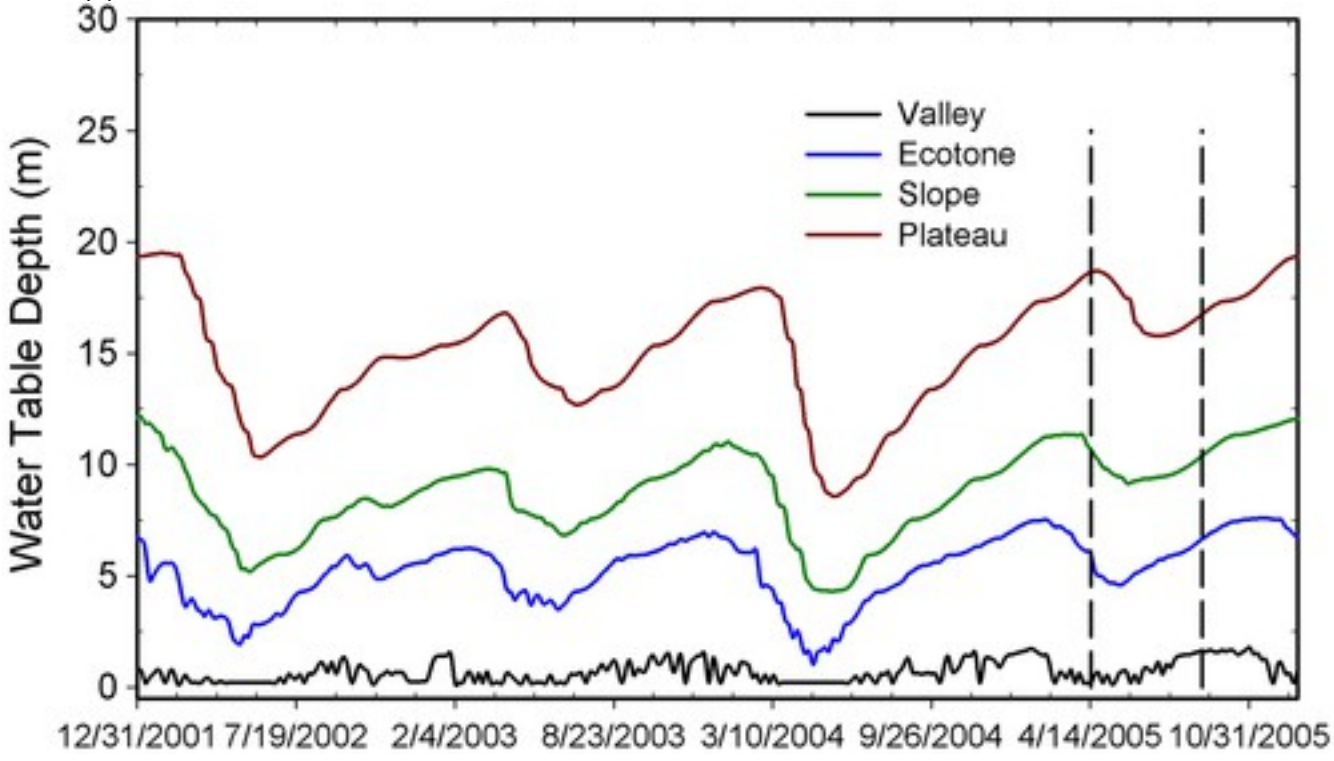

Figure 6

Open in figure viewerPowerPoint

Simulated interannual variability in water table depth at selected locations along x = 2,295 m for Case 3. The two dashed lines are 15 April 2005 and 2 September 2005, respectively.

To understand how processes controlling water movement in the plateau may differ from those along the slope, Figure 7 shows the pressure distribution at y = 2745 m (ecotone) and y = 1485 m (plateau). At the plateau (Figure 7a), water redistributes, driven by gravity, into the intermediate zone that is above the water table during both times in April and September. At the intermediate zone (Figure 7b), water redistributes in the zone above the water table by gravity in the wet season. In the dry season, capillary forces draw water up from the water table to supply water for the process of evapotranspiration, thus reducing the depth of the water table.

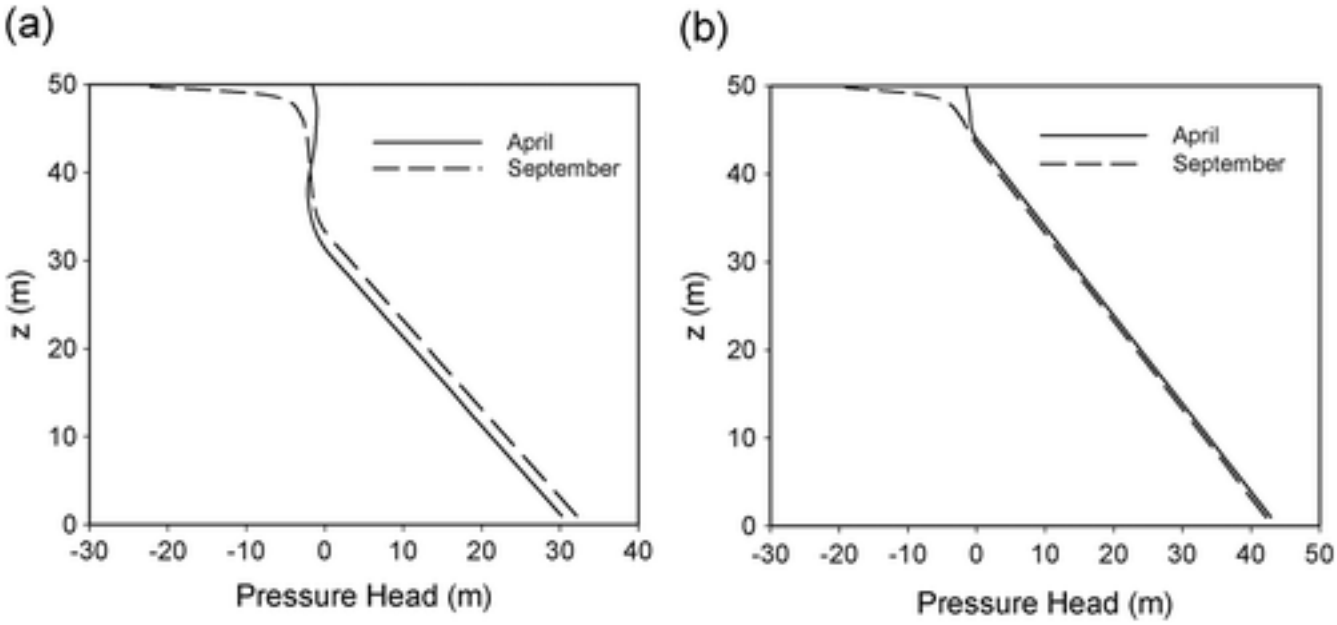

Figure 7

Open in figure viewerPowerPoint

(a, b) Vertical pressure profile at selected points along the cross section at x = 2,295 m for Case 3.

The default runoff parameterization used in Case 1 produces too much runoff in the wet season. Runoff for Cases 3 and 4 are comparable despite small differences in seasonal variation (Figure 4b). Runoff shows double peaks in the wet season, which are concomitant with the double peaks of rainfall as shown clearly in Figure 2. In Case 1 the peak of runoff is concomitant with the water table rise in April. This suggests that even though recharge is the same in the three simulations (Cases 1, 3, and 4), considering lateral flow and the interaction between groundwater flow and streamflow has important effects on the timing of runoff. In the dry season, runoff for Case 3 is closer to Case 4, and Case 5 is closer to Case 6, suggesting that the differences in runoff are more driven by boundary conditions than soil parameters.

Cases 5 and 6 have similar characteristics of WTD as Cases 3 and 4. Comparing the four ParFlow cases, it is evident that the WTD difference due to soil parameters is larger than the WTD difference between ParFlow driven by P-ET provided by ALM and ParFlow coupled to an earlier version of CLM. This is not surprising since the ET simulated in Case 1 is comparable to that simulated in Case 5 (Figure 2), as ET is mainly limited by energy. A lot of improvements including ET partitioning have been made in later versions of CLM, which is the predecessor of ALM. The ET in Case 5 is slightly lower than that in Case 1 due to these model improvements. Lower ET results in higher recharge rate compared to Case 3. Hence, the surface infiltration prescribed in Cases 3 and 4 should be a little smaller than the surface infiltration simulated in Cases 5 and 6, leading to differences in WTD between Case 3 and Case 5 (or Case 4 and Case 6) with the same soil parameters. Higher recharge rate also increases baseflow (Figure 4b), delaying the timing of runoff [*Price*, 2011]. Because of the delayed recharge dynamics at the plateau, the gradient from the plateau toward the valley is the maximum at the peak of the dry season and baseflow is increased at the end of the dry season.

Comparison of the ALM and ParFlow results indicates a dominant control of lateral processes on WTD and runoff. For example, there are substantial spatial variations in the WTD difference between Case 1 and Case 3 (Figure 8). As expected, including lateral flow, ParFlow simulates deeper water table depth at the plateau and shallower water table depth at the valley. Since 1-D models such as ALM do not explicitly represent lateral redistribution of water and the spatial distribution of WTD and runoff, a pertinent question is whether ALM could be tuned to reproduce the spatial mean behavior of WTD and runoff simulated by ParFlow without the model structural complexity to represent lateral redistribution. To address this question, we repeated Case 1 by adjusting the subsurface drainage decay factor that controls the water table depth by trial and error to match the long-term spatial average WTD of Case 3 (Figure 9a). The change of water table depth does not have effect on ET (not shown) for ALM, as also predicted by model simulation in *Miguez-Macho and Fan* [2012]. Therefore, this new Case 1 has the same P—ET as the original Cases 1 and 3. However, the change in subsurface drainage decay factor affects the peak arrival time of both groundwater table and runoff (Figure 9). We digitized the streamflow data in *Cuartas et al*. [2012] for 2005. Even without formal model calibration, the match between the observation and the 3-D simulation in streamflow amount and temporal dynamics for the third-order stream is satisfactory in the dry season (Figure 10). *Cuartas et al*. [2012] showed that the Asu catchment has a flux tower whose footprint coincides with the Asu catchment area, and the rainfall intensity measured by that flux tower is higher than that at the K34 flux tower. This may explain the general low bias in our model simulations driven by rainfall from K34 compared to observations. However, runoff arrival for the calibrated Case 1 is

delayed compared to Case 3 and baseflow is improved but still lower compared to the observations. This suggests that with parameter calibration, ALM may be able to reproduce the long-term spatial average WTD and runoff simulated by ParFlow, but without a representation of lateral processes and the recharge dynamics along the slope, the calibrated simulation may become more unrealistic in the runoff timing and partitioning between surface and subsurface runoff.

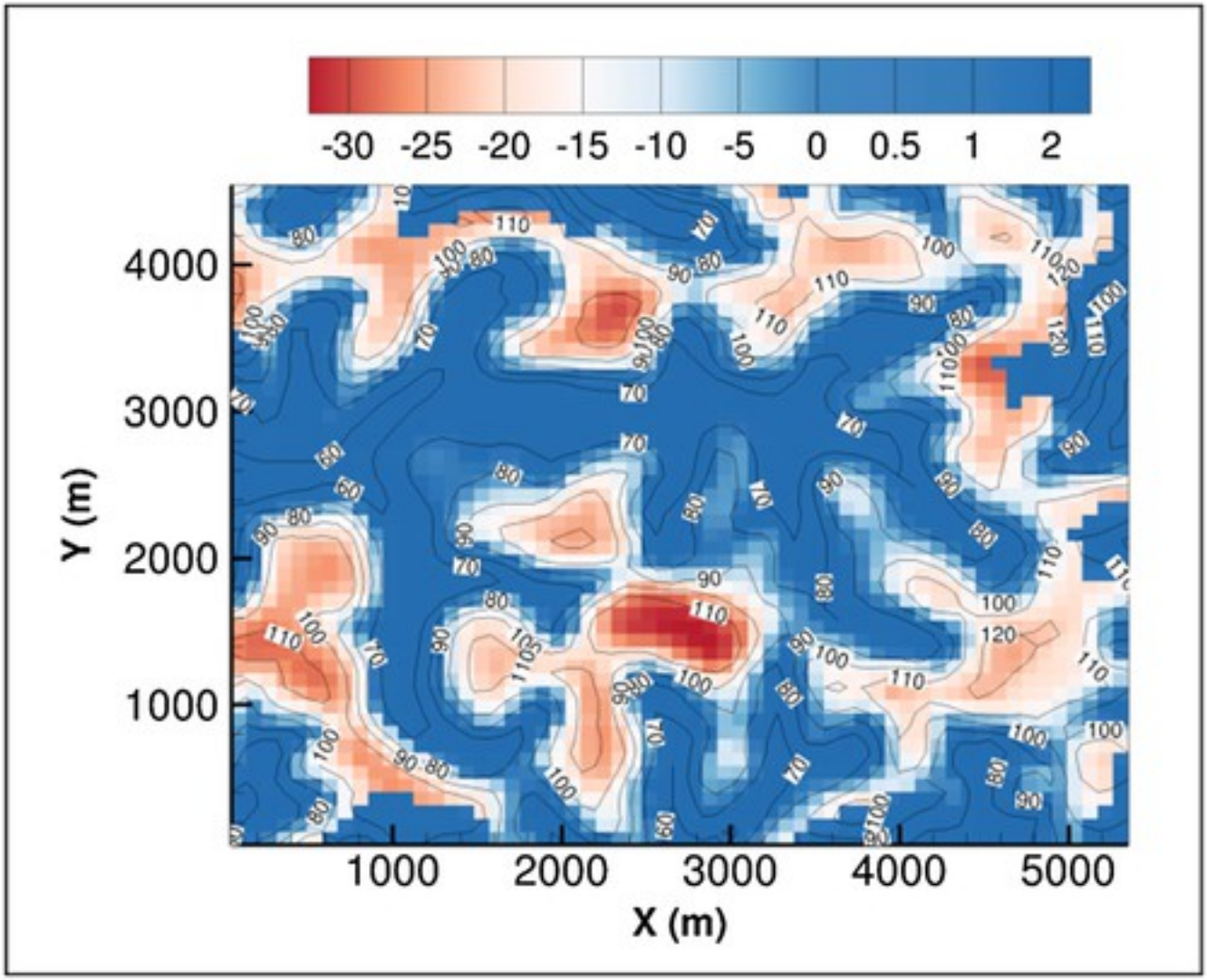

Figure 8

Open in figure viewerPowerPoint

Water table difference (m) between Cases 1 and 3 on 15 April 2005. The contour lines are the surface elevation.

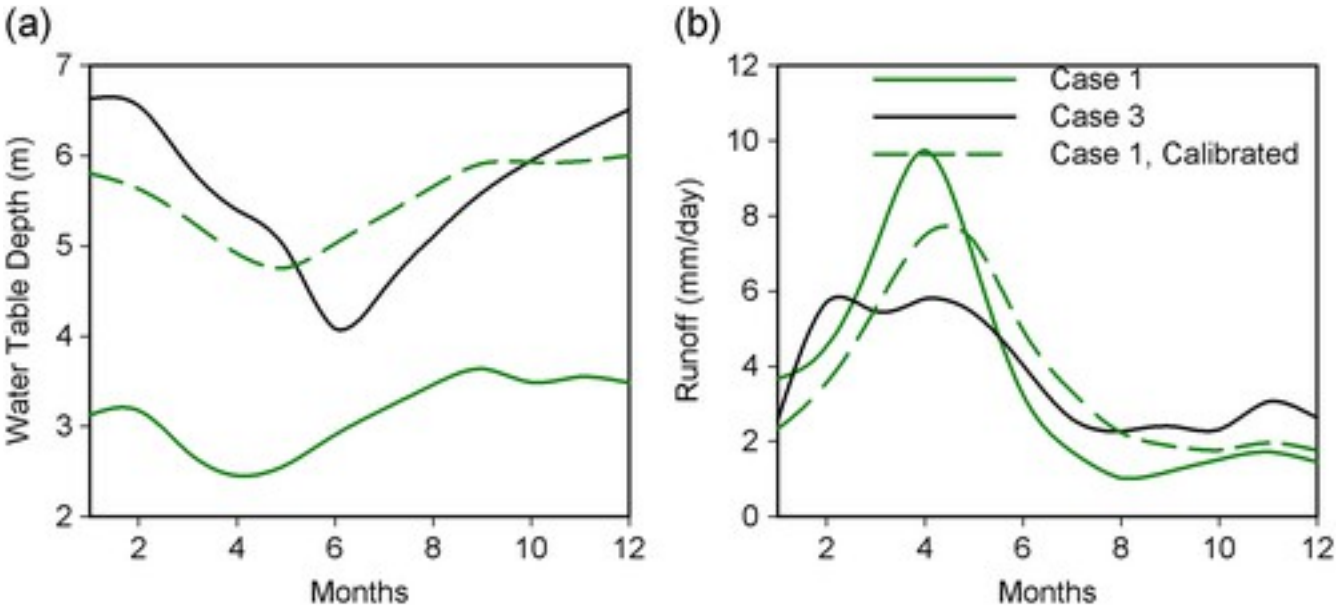

Figure 9

Open in figure viewerPowerPoint

Comparison of ALM simulations of (a) water table depth and (b) runoff, averaged over 2002 to 2005, in Case 1 with and without calibration with the simulation in Case 3.

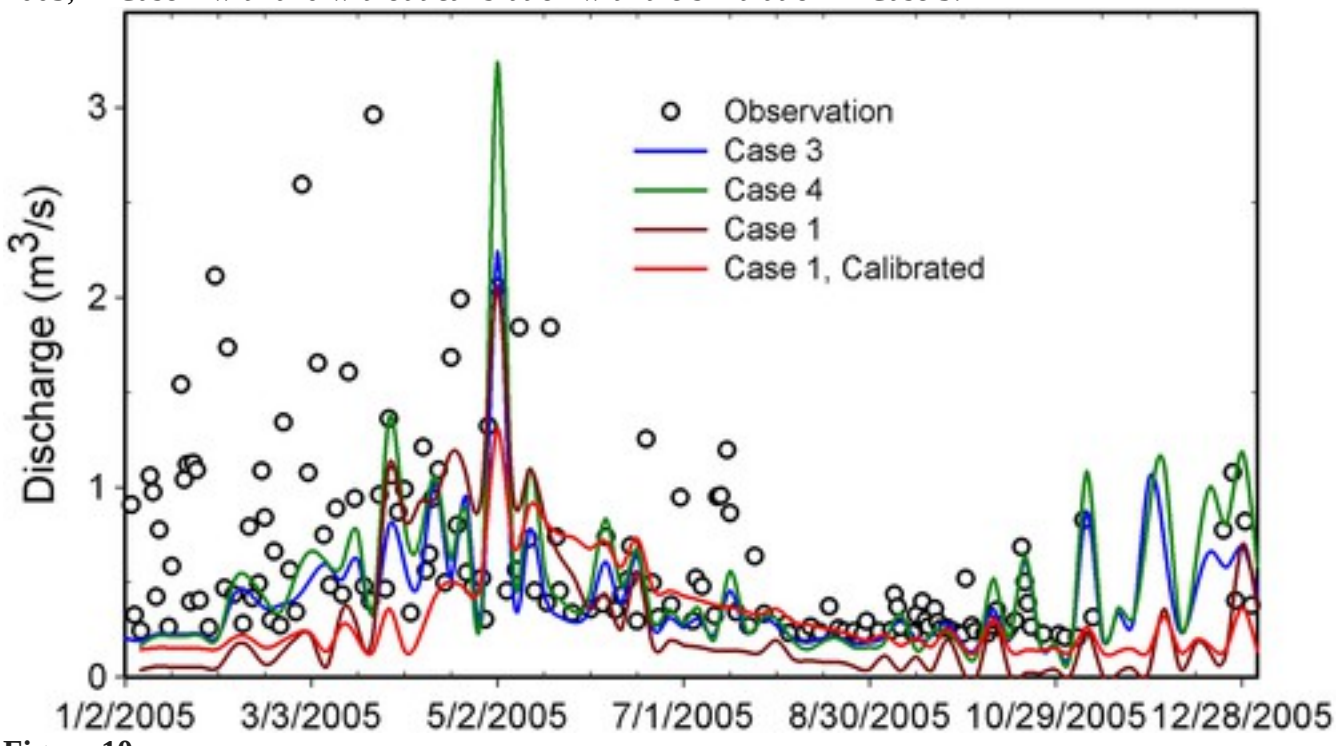

Figure 10

Open in figure viewerPowerPoint

Model comparison of streamflow for the third-order stream with observations.

3.4 Evapotranspiration

As shown in Figure 2, despite the large seasonal variation in precipitation, ET shows a very small seasonal variation, suggesting that the dry season ET at Asu is not limited by surface water supply, while the wet season ET is limited by radiation. The aridity index of the ASU site is 0.55, which also indicates that the site is energy limited. The root density profile specified in ALM and CLM-ParFlow suggests that 80% of the total demand of transpiration is supplied by the top meter of the soil and the top 4.0 m can satisfy the total transpiration demand. The root water uptake corresponding to this rooting depth is consistent with the observations in *Broedel et al.* [2017] at K34 during normal climatological years, when the total transpiration is supplied by the top 4.8 m soil water. To understand why the model-simulated ET is not limited by water in the Asu catchment, it is important to understand what controls transpiration in the models. In both ALM and CLM, stomatal conductance is affected by a wilting factor that depends on soil water matric potential in each soil layer in the top 4.0 m as follows [*Oleson et al.*, 2013]:

$$\beta = \frac{\psi_C - \psi_S}{\psi_C - \psi_O} \quad (7)$$

where β is the wilting factor, ψ_s is the soil water matric potential (m), ψ_c is the soil water potential (m) when stomata are fully closed, and ψ_o is the soil water potential (m) when stomata are fully open. $\beta = 1$ when vegetation is unstressed, and $\beta = 0$ when the plant wilting point is reached. The parameters ψ_o and ψ_c for broadleaf evergreen trees are −66 m and −255 m, respectively. Figure 11 shows the spatial distribution of saturation of the top soil layer simulated in Case 5 with the ALM soil parameters during the dry season of 2005 when the Amazon experienced drought. Surface topography has a strong influence on soil saturation, as indicated by the strong spatial correspondence between the two. The minimum saturation in the region is around 0.6, and the corresponding soil water matric potential from the soil retention curve (Figure 12a) is −20 m, which is less negative than ψ_o. Similarly for Case 6 using the C12 soil parameters, Figure 12b shows that at the plateau during the same time period, the soil water matric potential that corresponds to the lowest saturation is also less negative than ψ_o. These model results suggest that even during the dry season of the 2005 drought year and considering uncertainty in soil parameters, the simulated soil saturation is high enough that the stomata are fully open, so transpiration is not water limited.

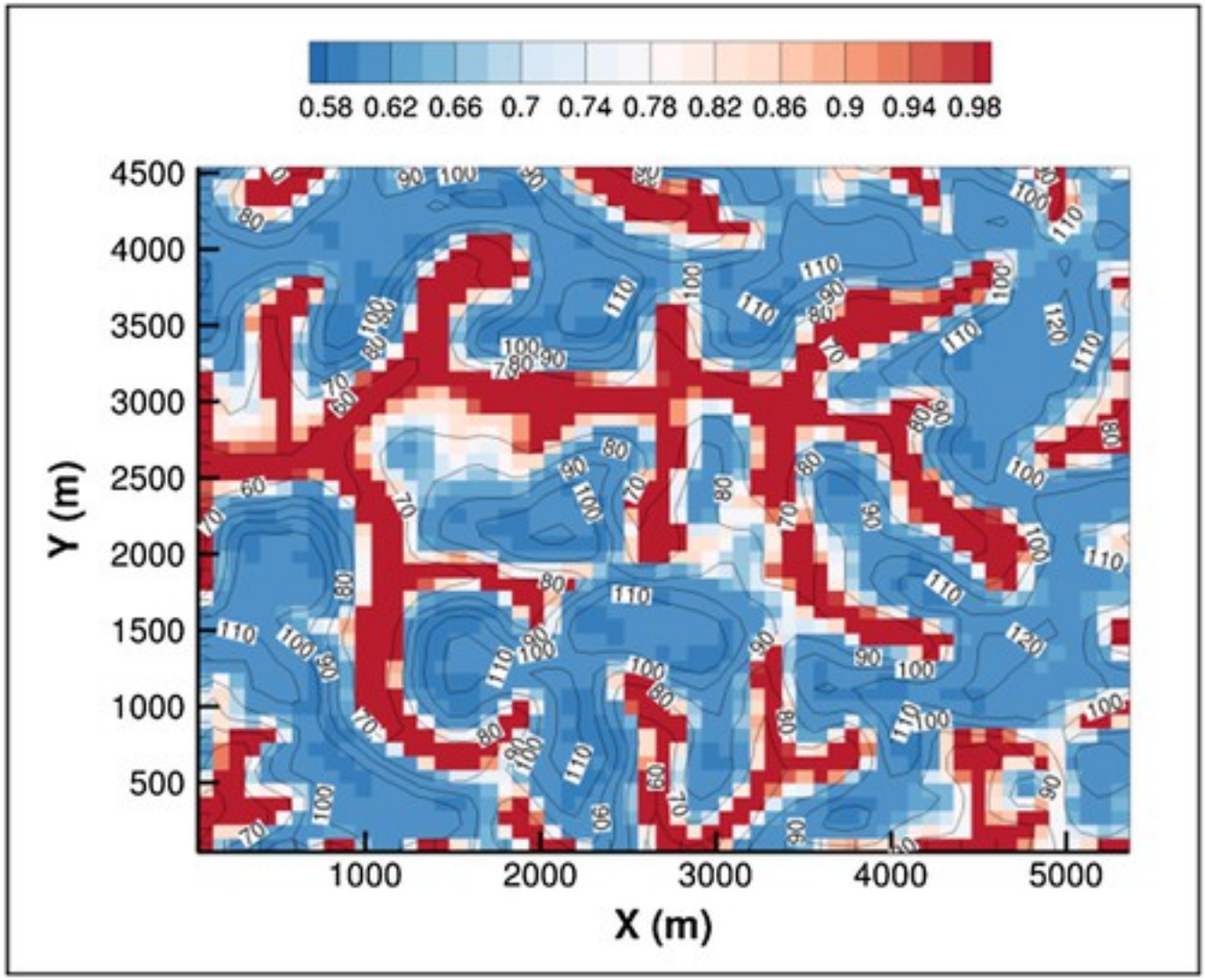

Figure 11

Open in figure viewerPowerPoint

Spatial plot of soil saturation of top soil simulated in Case 5 on 5 September 2005. The contour lines are the surface elevation (m).

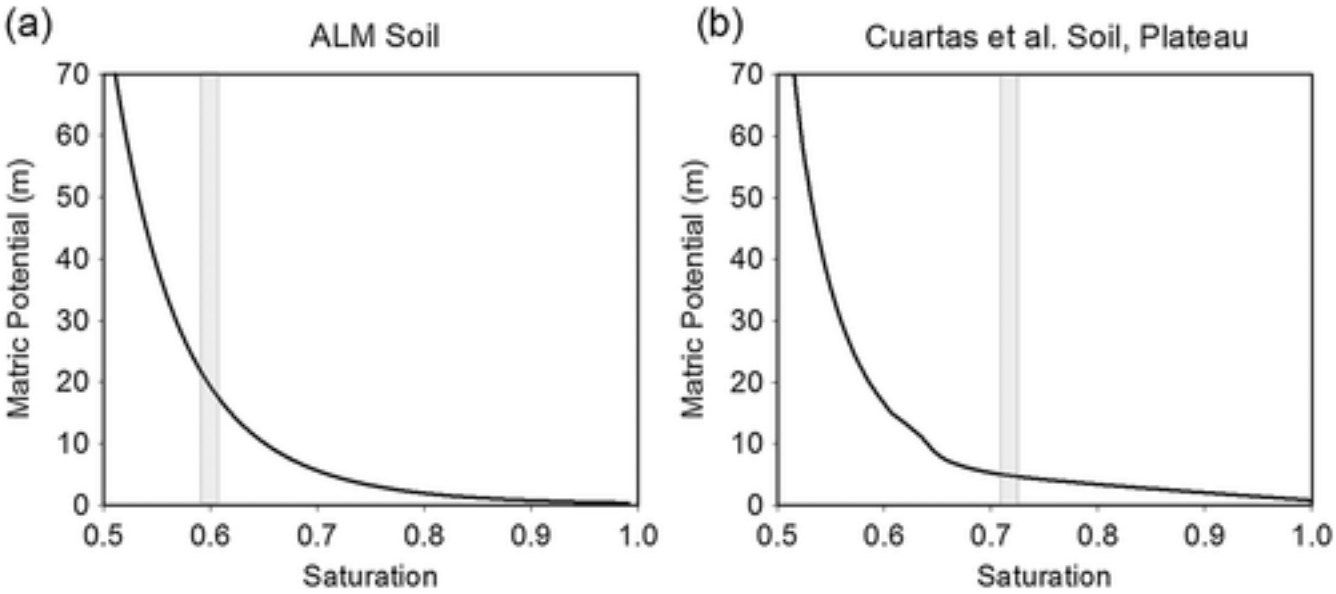

Figure 12

Open in figure viewerPowerPoint

Water retention curves for the (a) ALM soil and (b) C12 soil. The shaded area shows the lowest saturation simulated by ParFlow using the corresponding soil parameters.

Figure 13 shows the spatial distribution of ET simulated by CLM-ParFlow as influenced by the spatial distribution of groundwater table, which is deeper at the plateau and shallower at the valley. As mentioned earlier, transpiration at the Asu catchment is not water stressed, and stomatal responses caused by root hypoxia is not considered, so it is spatially uniform and not shown. However, ground evaporation depends on soil water as shown in Figure 13a, which results in a higher *T*/ET ratio in the morning of a selected day (Figure 13b) in the plateau where groundwater table is deep. This behavior is consistent with the finding in *Maxwell and Condon* [2016], but it cannot be predicted by the 1-D ALM or CLM without representations of lateral processes.

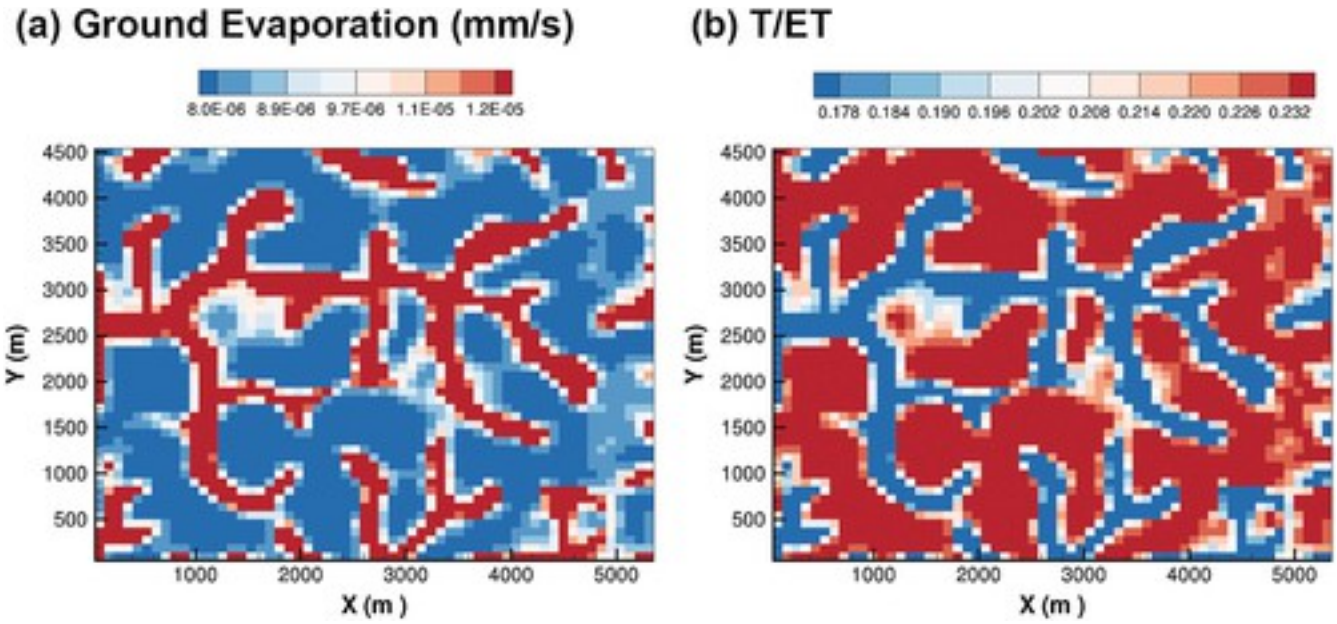

Figure 13
Open in figure viewerPowerPoint
Spatial distribution of (a) ground evaporation and (b) the *T*/ET ratio in the morning of 15 September 2005 for Case 5.

3.5 Sensitivity Analysis

To determine the sensitivity of the findings derived from the ALM and ParFlow simulations discussed above, we further explored other factors that may introduce simulation uncertainty. To this end, sensitivity analysis was performed by changing the bedrock depth at which the lower boundary condition is imposed and anisotropic ratio of hydraulic conductivity that may influence the seasonality and spatial variability of WTD and runoff, and by changing the atmospheric forcing that may influence the seasonality of evapotranspiration. These experiments will allow us to explore uncertainty in simulating water availability and evapotranspiration that sustain plant functioning in the dry season and under drought. As mentioned in section 3.1, these experiments were selected to answer the two key questions of this study. As to how much water is available to plants depends on the soil depth, hence water storage, Case 3 was repeated with a different bedrock depth. Although bedrock depth may change the patterns of groundwater flow, varying the bedrock depth for Case 3 by 5 m did not produce noticeable change in the flow pattern (not shown).

How much water is available to tropical forest also depends partly on the atmospheric forcing that determines whether the hydrologic regimes are limited by energy or water. To explore uncertainty related to atmospheric forcing, we repeated the simulations of Cases 1 and 3 by adopting all of the relevant atmospheric forcing from the K34 flux tower, in contrast to the

experiments in Table 2 that were forced by the K34 rainfall in combination with radiation and other forcing data from the Princeton's Global Meteorological Forcing Data set. Seasonal ET simulated by the K34 forcing is reduced, with a maximum reduction of 9.7% of the simulation with the Princeton forcing. Water table is shallower with the K34 forcing, especially in the dry season, while total runoff is not affected too much (see Figure S1 in the supporting information). K34 flux tower has a few independent estimations of latent heat fluxes by the eddy correlation method in 2005. Figure 14 compares the ET calculated from the latent heat fluxes and the simulated diurnal ET variations over a 7 day period in May (Figure 14a), August (Figure 14b), and December (Figure 14c) when measurements are available. Both simulations show higher ET in the dry season compared to the wet season, consistent with the variability observed from the flux tower measurements in the Amazon [*Kim et al.*, 2012]. Without calibration, ET variations from the simulation using the K34 forcing agree well with the observation, indicating that realistic data such as incoming solar radiation is important to correctly simulate ET. The seasonal fluctuation of runoff does not change much. Using the P-ET from the ALM simulation with the K34 forcing, Case 3 was executed. The K34 forcing resulted in an increase of water table fluctuation by 0.21–0.3 m and the runoff slightly increases (see Figure S2 in the supporting information). Therefore, uncertainty in atmospheric forcing has some effects on the magnitude of ET, WTD, and runoff, but the effects on the seasonal variations and timing are inconspicuous.

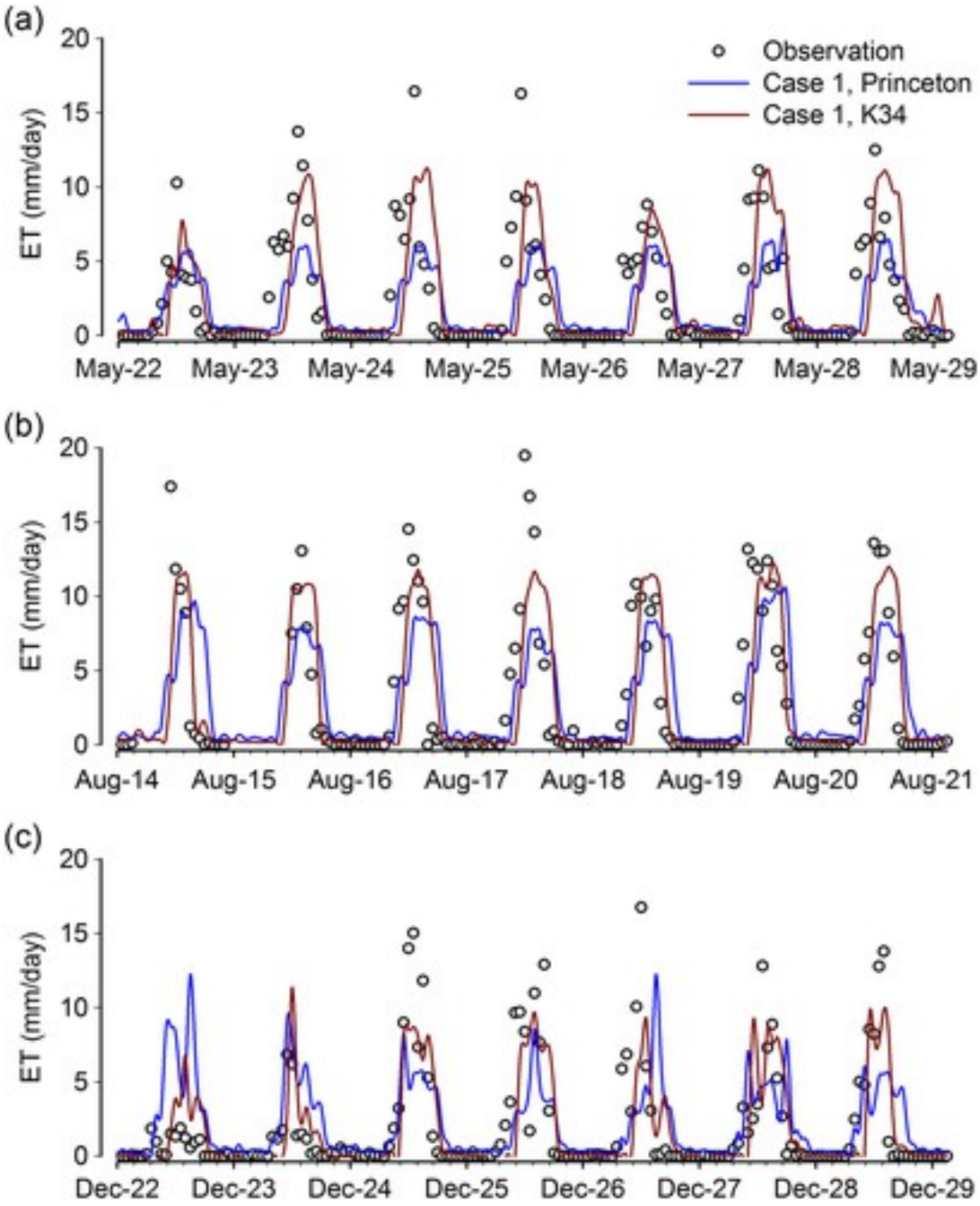

Figure 14

Open in figure viewerPowerPoint

Diurnal variation of observed and simulated ET from Case 1 using different forcings during a 7 day period in (a) May, (b) August, and (c) December 2005.

Soil hydraulic conductivity is usually anisotropic, i.e., direction dependent. Anisotropy is important in simulating land drainage. The soil in central Amazon is dominated by macropores under primary forest [*Chauvel et al.*, 1991], which may result in high lateral hydraulic conductivity. From the analysis of simulation results, it has been shown that lateral flow processes simulated by the 3-D ParFlow model is a key factor responsible for the difference

between 1-D ALM and 3-D ParFlow simulations. Therefore, another simulation that varies the anisotropy of soil conductivity was conducted to determine the sensitivity of the lateral processes and available water for plants to anisotropy. We repeated Case 5, changing only the anisotropy of the hydraulic conductivity by using a ratio of 10 for K_h/K_v. For simplicity, the ratio is uniform along the soil depth, even though a gradual reduction of macropores with soil depth is observed at a nearby site [*Broedel et al.*, 2017]. Increasing the anisotropy ratio significantly enhances the process of subsurface lateral flow, increasing the water table depth and baseflow (see Figure S3 in the supporting information). Under this scenario, the water table depth is so deep that the interactions of unsaturated-saturated zone are insignificant at the plateau. The plant available water capacity of the soil for this case is the lowest among all the cases. However, the soil matric potential is still less negative than that needed to maintain fully open stomata, meaning that there is plenty of soil moisture for the plant to extract for transpiration. Similar spatial *T*/ET ratio as in Case 5 (Figure 13b) was predicted but not shown.

4 Discussion

To better understand how tropical forests respond to drought requires an improved ability to accurately predict the spatial variability in water table and soil moisture available for plant use. Model simulations of surface water-groundwater interactions suggest the likely importance of the groundwater to the Amazon water cycle by buffering the soil water stress [*Miguez-Macho and Fan*, 2012; *Pokhrel et al.*, 2014]. Reviewing the development history of ESMs, *Clark et al.* [2015] summarized many key opportunities to improve hydrologic process representations in LSMs used in ESMs. Examples include (1) explicit representation of variably saturated flow using the mixed form of Richards' equation, (2) explicit representation of macropore and fracture flow, (3) explicit representation of hydraulic gradients throughout the soil-plant-atmosphere continuum, (4) explicit representation of stream-aquifer interactions, and (5) improved data sets of soil type, soil parameters, bedrock depth, etc. They also emphasized the strong need for a systematic and controlled approach for model evaluation in order to understand model development needs and identify modeling alternatives without significantly increasing the computational burden.

By systematic design of numerical experiments using models of different structures, i.e., ALM and ParFlow, and model soil parameters, we were able to identify through ParFlow that spatial heterogeneity in soil and topography has evident impact on soil hydrology. ALM cannot capture features such as the delayed groundwater recharge at the plateau that can be simulated by ParFlow. ALM cannot reproduce the seasonal and spatial variations of WTD and runoff simulated by ParFlow despite successful tuning of an ALM model parameter to reproduce the

long-term spatial average WTD simulated by ParFlow. Clearly, there is a need in ALM to take small heterogeneity and subsurface hydrological processes into account.

Soil parameters do not have much impact on ET and runoff simulated by ALM. However, those parameters cause larger differences in water table depth simulated by ParFlow than the imposed top boundary conditions, i.e., P-ET from ALM, P-ET from direct coupling with CLM, or P-ET from different sources of atmospheric forcing. The seasonal discrepancy between WTD and runoff from ALM and ParFlow indicated the importance of lateral flow that is currently missing in ALM.

Lack of physical constraints can lead to false drought response for ecosystem models [*Sperry and Love*, 2015]. At the Asu catchment, transpiration is not water stressed in any 1-D or 3-D model simulations analyzed in this study. Although landscape heterogeneity has important effects on groundwater storage and runoff, our simulations show that ET is not water limited even during the dry season in the 2005 drought year in the plateau regions of the Asu catchment where groundwater table is evidently deeper compared to the valley. Furthermore, this finding is not sensitive to uncertainty in atmospheric forcing and soil parameters although these factors have noticeable effects on the soil hydrology. We note, however, that the current empirical formulation of the wilting factor (equation 7) is a key parameter that determines the minimum soil saturation for the stomata to respond to water stress. In other words, the wilting factor is crucial to accurately estimate how soil water stress affects transpiration. A number of wilting factor formulations have been proposed [*Verhoef and Egea*, 2014]. Due to the lack of long-term soil moisture and streamflow records and the lack of evidence for whether the forest experiences moisture stress during prolonged dry conditions, we are not able to validate which formulation is more representative.

Our simulations of higher ET in the dry season than the wet season (Figure 2) are consistent with the sensible and latent heat flux measurements across a biome gradient in Brazil, showing that coincident with increased radiation, evaporation rates increased in the dry season in Amazon sites such as Manaus near the Asu catchment where annual precipitation is above 1900 mm and the dry season length is less than 4 months [*da Rocha et al.*, 2009]. Analyzing 11 years (including major drought events in 2005 and 2010) of dry season (July–September) Moderate Resolution Imaging Spectroradiometer (MODIS)-enhanced vegetation index (EVI), and normalized difference vegetation index (NDVI) images, *Atkinson et al*. [2011] found that the response of Amazon vegetation to drought is not detectable through satellite-observed changes in vegetation greenness. However, daily ET calculated from the flux tower measurement is low in 2005 compared to the potential evapotranspiration calculated using the forcing at the K34 flux

tower and the Penman-Monteith equation [*Allen et al.*, 1998] standardized by the Food and Agriculture Organization (FAO-56 method), suggestive of possible drought stress (Figure S4). The potential inconsistency highlights important uncertainty in evaluating drought stress using different measurements and analysis/modeling methods. Potentially, for more intense and prolonged drought with annual precipitation less than 1900 mm for an extended period, water stress could play a more important role in tropical forest response to drought, especially in the plateau with deeper groundwater table as shown in our simulations. In the future, we will investigate this issue further using more extensive measurements of the 2015–2016 El Niño-related Amazon drought and modeling that includes (1) detailed aquifer-stream interactions, (2) representations of plant hydraulics including plant water storage and hydraulic redistribution [*Oliveira et al.*, 2005] coupled to soil hydrology, and (3) the effect of the macropores contributing to, for example, preferential flow, the hysteresis in soil moisture characteristics under wetting and drying processes [*Miguel and Vilar*, 2009], etc. to improve our understanding of hydrological processes in the catchment.

Lastly, 3-D distributed, process-based hydrological models are not often applied at larger spatial extents due to the lack of input data and the computational burden, numerical instability and convergence issues. This reinforces the need to develop approaches in ESMs to be able to simulate key representation of hydrologic processes such as lateral flow that has dominant influences on surface and subsurface water dynamics while maintaining computational efficiency. Recent efforts to explore a new subgrid structure in ALM to represent subgrid topographic variations [*Tesfa and Leung*, 2017] provide a useful modeling framework for developing parameterizations of lateral processes driven by surface topography. For example, the subgrid framework of ALM may be combined with the hybrid 3-D hillslope hydrological model [*Hazenberg et al.*, 2015] where lateral responses are aggregated to the topographic land units of ALM to provide a more computationally efficient method than 3-D distributed models for simulating both vertical and lateral hydrologic processes in Earth system models. Developing approaches to represent lateral processes, in addition to incorporating plant hydraulics and preferential flow discussed above, are key efforts needed to improve the ability of Earth system models in simulating tropical forest response to drought and the future of the land carbon sink under climate change.

Acknowledgments

This work was supported by the U.S. Department of Energy Office of Biological and Environmental Research as part of the Terrestrial Ecosystem Systems program through the Next

Generation Ecosystem Experiment (NGEE) Tropics project. The data used for model simulations are listed in the tables and all input data and model outputs are archived on the computers at PNNL and will be available upon request by contacting Yilin Fang (yilin.fang@pnnl.gov). A portion of this research was performed using PNNL Institutional Computing at Pacific Northwest National Laboratory. PNNL is operated for DOE by Battelle Memorial Institute under contract DE-AC05-76RL01830.